Pergamon

Journal of Structural Geology, Vol. 19, No. 2, pp. 209 to 224, 1997

PII: S0191-8141(96)00058-2
0191-8141/97 $17.00 + 0.00

Timing and nature of magmatic fabrics from structural relations around stoped blocks

T. KENNETH FOWLER JR* and SCOTT R. PATERSON

Department of Earth Sciences, University of Southern California, Los Angeles, U.S.A.

(*Received* 27 *July* 1995; *accepted in revised form* 9 *July* 1996)

Abstract—Structural relations around several large (> 100 m) stoped blocks in the granodiorite of Castle Creek, Sierra Nevada, California, suggest that magmatic fabrics formed as or after the space-making phase of pluton emplacement had ended. The stoped granite blocks are approximately 360 m below the exposed pluton roof. Magmatic foliations in granodiorite surrounding the blocks commonly follow km-scale orientation trends to within 1 m of block contacts, where they become deflected parallel to the block boundaries. Locally, undeflected foliations occur within a few centimeters of block contacts. Mafic enclave fabric ellipsoid intensities ($0.2 < Es < 0.7$) and shapes (mostly plane to oblate) show little relation to distance from stoped block contacts. Mineral and enclave linear fabrics vary widely in orientation. In short, magmatic fabrics in the granodiorite of Castle Creek show virtually no strain record for sinking of these presumably late, stoped blocks. Instead, these fabrics reflect shortening of the surrounding granodiorite magma associated with the formation of km-scale fabric trends.

We draw the following conclusions concerning magmatic fabrics in the granodiorite of Castle Creek: (1) magmatic fabrics formed during and/or after the latest stages of pluton emplacement, and thus, contain little or no information about space-making processes; (2) magmatic fabrics had poor strain memory; and (3) during magmatic fabric formation, pluton strains were partially decoupled from host-rock strains. Published data from other plutons indicate that these relationships may be common, particularly in the brittle upper crust. It follows from these conclusions that even in the best case, magmatic fabrics contain only qualitative information about pluton emplacement mechanisms, regional tectonics, and internal magma chamber processes. Interpretations of magmatic fabrics must be corroborated by evaluating causes, kinematics, and magnitudes of syn-emplacement host-rock deformation. In the worst case, the causes of magmatic fabrics cannot be uniquely determined. © 1997 Elsevier Science Ltd. All rights reserved

INTRODUCTION

The pioneering work of Cloos (1925) led to widespread recognition of the importance of magmatic fabrics for understanding pluton emplacement and processes within magma chambers. Recent progress has centered on the conditions of magmatic fabric formation, with an emerging consensus that alignments of igneous minerals and mafic enclaves in plutons record strain, during crystallization, of a rheologically complex mush containing crystals and melt (Marre, 1986; Pitcher, 1993). Experimental work on partially melted rocks has helped to constrain the rheological behavior and deformation mechanisms of granitic magmas (Arzi, 1978; van der Molen and Paterson, 1979; Dell'Angelo *et al.*, 1987; Laporte, 1994; Rushmer, 1995). The relationship between strain and magmatic fabric geometry has been investigated via field studies, and analog and mathematical simulations (Blumenfeld and Bouchez, 1988; Fernandez, 1988; Ildefonse *et al.*, 1992; Nicolas *et al.*, 1993; Tikoff and Teyssier, 1994a). Means and Park (1993) and Park and Means (in press) have utilized a thin-section shearing device to directly observe dynamic strain and recovery processes in a deforming, non-silicate crystal/melt mush. Microstructural criteria for the recognition of melt-present fabrics in granitic rocks have been presented by Hutton (1988a), Blumenfeld and Bouchez (1988), and Paterson *et al.* (1989).

In contrast, relatively little progress has been made in deciphering the causes of magmatic fabrics in plutons; the fundamental problem being that different processes can produce similar fabric geometries. Magmatic fabrics have been variously interpreted to form as the result of pluton ascent and/or emplacement, regional tectonic strain, and internal magma chamber processes. Hypothesized emplacement-related processes include magma strain within an ascending diapir (Dixon, 1975; Ramberg, 1981; Schmeling *et al.*, 1988; Cruden, 1990), or during *in-situ* ballooning, accommodated by either forcible displacement of the host rock envelope (Holder, 1979; Ramsay, 1989; Brun *et al.*, 1990) or by passive fault-controlled dilation (Guineberteau *et al.*, 1987; Hutton, 1988b). During crystallization, hot, easily-deformed plutons should be sensitive indicators of regional tectonic strains and magmatic fabrics have been used to interpret regional strain fields at the time of emplacement (Archanjo *et al.*, 1994; Tobisch *et al.*, 1995; Bouchez and Gleizes, 1995; Vauchez *et al.*, 1995). Potential internal fabric-forming processes include convection (Barriere, 1981; Phillips *et al.*, 1981; Stephens, 1992), magma surges (i.e. redistribution of magma within the pluton without growth of pluton size), and addition or removal of magma from the chamber (open system behavior). Thus, models of pluton emplacement and magma chamber evolution critically depend upon the interpreted causes of magmatic fabrics.

Three uncertainties impede determination of the causes of magmatic fabrics. First, similar foliation and lineation map patterns can be produced by different

*Present address: Exxon Production Research Company, P.O. Box 2189, Houston, TX 77252-2189, U.S.A.

causes. Second, magmatic strains can be mechanically decoupled from host rock strains. Third, it is often difficult to assign precise timing of fabric formation relative to particular ascent, emplacement and post-emplacement processes. For example, magmatic foliations and mafic enclaves in many plutons define a concentric map pattern characterized by radially-increasing shortening strains normal to the pluton contact and extensional strains parallel to the contact. Many previous workers have attributed these strain fields to inflation of a ballooning magma chamber (Holder, 1979; Bateman, 1985; Ramsay, 1989). However, concentric foliation patterns could instead represent convection, or deformation of early magma batches by later magma pulses or surges inside a pluton of fixed size (Schmeling *et al.*, 1988; Cruden, 1990; Paterson and Vernon, 1995). The mechanical contrast between granitic magma and its solid host rock may partially decouple pluton and host rock strain fields, particularly in the brittle upper crust. Stress and strain refraction at the rheological boundary could induce contact-parallel magmatic structures regardless of the cause of magmatic strain. Problems related to timing also bear strongly on interpretations of magmatic fabrics; these fabrics can potentially post-date the space-making phase of pluton emplacement. As a final complication, magmatic fabric patterns may not record the strain state from a single moment in time. Due to marginal cooling, magmatic fabrics should form diachronously as the crystallization front migrates inward from the pluton contact (Marsh, 1989; Bergantz, 1991).

Field data can help resolve these difficulties in the following ways: (1) by allowing correlation of pluton and host rock structures to test for any causative links in their formation; and (2) by establishing relative timing of fabric formation with respect to specific emplacement processes and internal structures (e.g. internal contacts, compositional layers, dikes, etc.). In this paper we describe structural relations between some stoped blocks and magmatic fabrics in the surrounding pluton (Pitcher, 1993). We infer that detachment and sinking of the blocks occurred late in the emplacement history. We argue that map-scale magmatic fabric patterns in the pluton formed during and/or after the time that these (presumably) late, stoped blocks sank to their present position. We then discuss the implications of these and other data for the interpretation of magmatic fabrics. We conclude that at least in this case (and possibly in many cases): (1) magmatic fabrics may form too late to record pluton emplacement (space-making) mechanisms; (2) magma strain memory is very poor; (3) pluton and host rock strains are at least partially decoupled and pluton and host rock structures evolve independently. If these interpretations are correct, it follows that even in the best case, magmatic fabrics contain only qualitative information about pluton emplacement, regional tectonics and magma chamber processes, and that in the worst case, the causes of magmatic fabric formation cannot be uniquely determined.

GEOLOGICAL SETTING OF THE STOPED BLOCKS

The study area lies within the voluminous Cretaceous portion of the Sierra Nevada batholith in Sequoia National Park, California (Fig. 1). Here, Sisson and Moore (1984) and Moore and Sisson (1987) have shown that the older granite of Lodgepole ($\geq$115 Ma; U–Pb; Chen and Moore, 1982) was intruded by younger granodiorite plutons of the Mitchell Intrusive Suite. The Mitchell Intrusive Suite consists of the granodiorite of Castle Creek (98 $\pm$ 2 Ma; U–Pb; Busby-Spera, 1983), the coarse-, and fine-grained facies of the Mitchell Peak granodiorite (91 Ma; U–Pb; Chen and Moore, 1982), and locally, a slightly younger, compositionally-layered border zone of aplite and schlieren that intrudes shallowly-dipping roof contacts between the granite of Lodgepole and Mitchell Intrusive Suite. Within the study area (Figs 2 & 3), the granodiorite of Castle Creek comprises two textural facies, a medium-grained facies with relatively few mafic enclaves (granodiorite of Castle Creek 1), and a slightly coarser-grained facies with abundant mafic enclaves (granodiorite of Castle Creek 2). The emplacement level for the Mitchell Intrusive Suite is loosely constrained, but probably lies near 8–10 km depth. Myriolitic cavities occur in both the granite of Lodgepole and the border phase of the Mitchell Intrusive Suite plutons. Immediately west of the Mitchell Intrusive Suite, aluminum-in-hornblende barometry from the Giant Forest granodiorite (97–102 Ma; U–Pb; Chen and Moore, 1982) suggests emplacement at 2.5–3.0 kilobars pressure, whereas 25 km to the east, the granodiorite of Lone Pine Creek was emplaced at

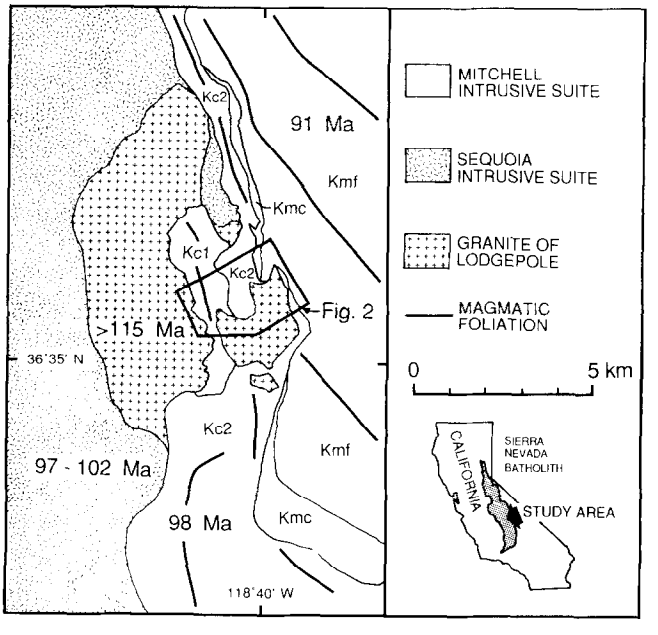

Fig. 1. Map showing location of study area. Units indicated within Mitchell Intrusive Suite are: Kc1 = granodiorite of Castle Creek 1; Kc2 = granodiorite of Castle Creek 2; Kmc = coarse-grained Mitchell Peak granodiorite; Kmf = fine-grained Mitchell Peak granodiorite. Magmatic foliations dip subvertically.

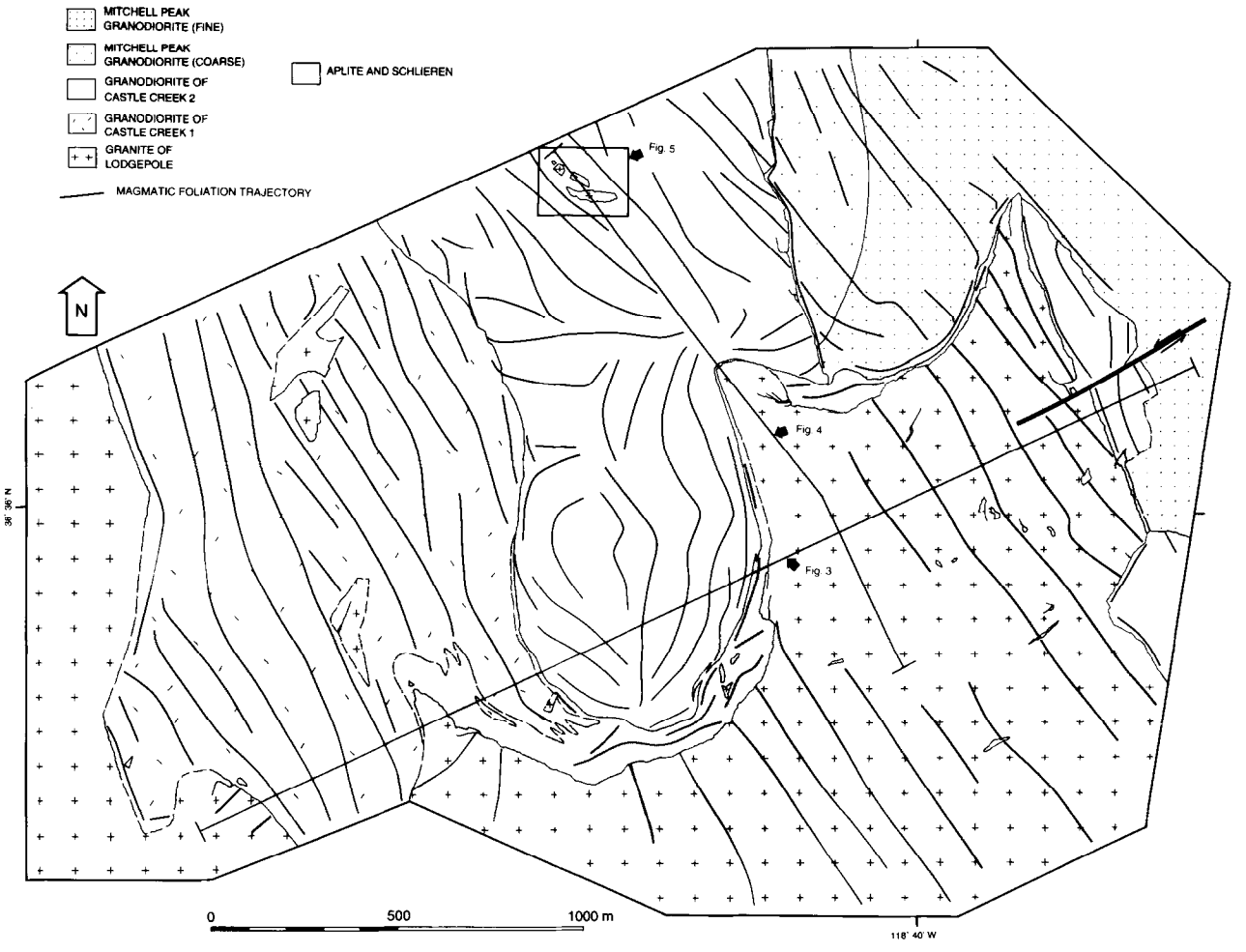

Fig. 2. Map showing geological setting of the stoped blocks. Trend lines show trajectories of magmatic foliation in the Mitchell Intrusive Suite, and of compositional banding (schlieren) in the granite of Lodgepole. The diagram is constrained by over 400 map stations (Fowler, 1996).

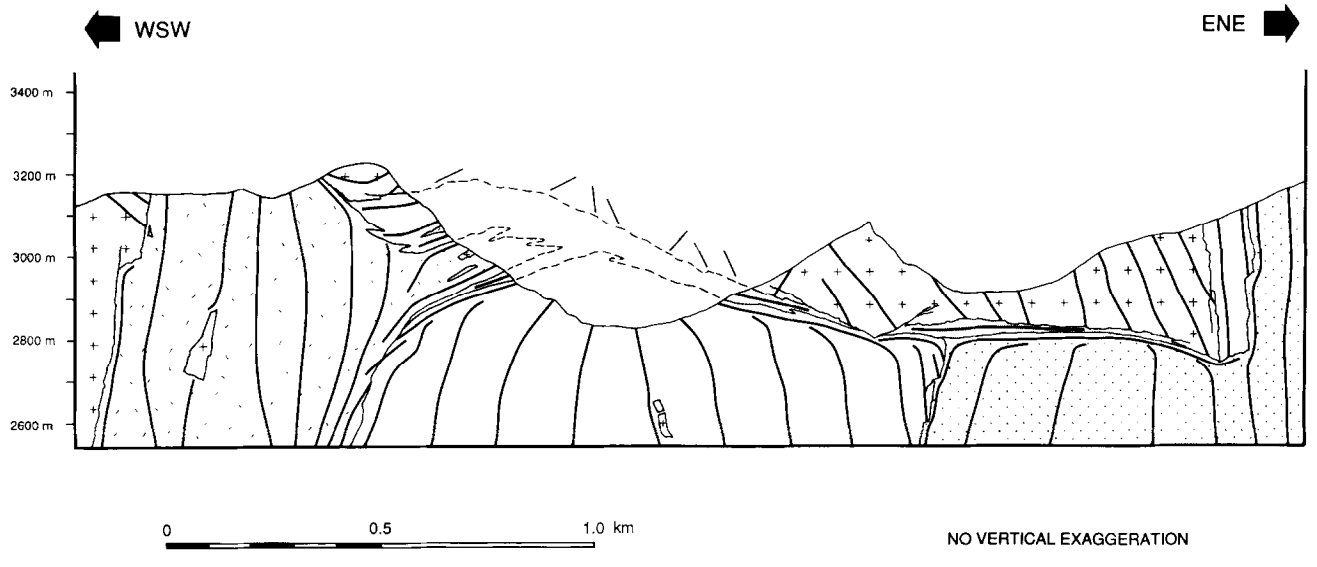

Fig. 3. Geological cross section showing internal structures and contact relations between the granite of Lodgepole and the Mitchell Intrusive Suite. All relations shown are exposed and have been projected laterally on to the line of section. Note that structural trends in the granite of Lodgepole are sharply truncated at intrusive contacts with the Mitchell Intrusive Suite, and that magmatic fabrics in Mitchell Intrusive Suite plutons are generally parallel to intrusive contacts within tens of meters distance. Map unit patterns are the same as in Fig. 2.

approximately 2.3–2.7 kb pressure (Ague and Brimhall, 1988).

The structural geology of the Lodgepole and Mitchell Peak plutons is described by Sisson and Moore (1984), Moore and Sisson (1987), and Fowler (1994a, 1996). Largely on the basis of contact relationships, Fowler (1994a, 1996) argues that magmatic stoping was the dominant process during final emplacement of the Mitchell Intrusive Suite. Intrusive contacts along the roofs and walls of these plutons are brittle fractures that discordantly cut all structures and fabrics in the older granite of Lodgepole (Figs 2 & 3). There is little evidence for assimilation or penetrative deformation of the granite host, for shearing of pluton contacts, or for coincidence of intrusive contacts with regional faults. In short, host-rock material cannot be area-balanced in map- or cross-section views; large amounts of host-rock are missing. The missing material is inferred to have been transported downwards out of the map plane by stoping.

The granodiorite of Castle Creek locally contains large stoped blocks of granite of Lodgepole. Map relations indicate that the granite xenoliths shown in Figs 2 and 4 are almost certainly detached from the main mass of the granite of Lodgepole and lie far below the pluton roof contact. The cross section is constrained by spectacular 3-dimensional exposures across two alpine cirque basins. Projection of the roof contact to a position above the blocks suggests that they have detached and sunk approximately 360 m, a distance equal to several times the radius of the blocks. Although it is possible to draw a cross section in which the blocks are still attached to the roof, it is unlikely that this is the correct interpretation because: (1) the roof contact consistently dips 10°–30° southeast for several kilometers of mapped exposure (Figs 2 & 3; Sisson and Moore, 1984), only showing steps and irregularities at a scale $\leq$50 m — attaching the blocks to the roof would require a significant departure from the observed contact orientation and style; and (2) the blocks have moved relative to one another (see below).

We infer that sinking and arrest of the stoped blocks was one of the final events in emplacement of the granodiorite of Castle Creek. Examination of Figs 2 and 3 indicates that preserved granite xenoliths, which make up $<1\%$ of the outcrop area of the granodiorite of Castle Creek, account for only a small fraction of the host-rock material that has been removed along discordant intrusive contacts. We suggest that the missing host rock material detached and sank relatively early during granodiorite crystallization, when the magma had correspondingly low density, viscosity and yield strength. Arrest and preservation of stoped blocks was possible only during later stages of magma crystallization, after magma density and mechanical strength had increased to some critical value. Thus, the preserved stoped blocks are interpreted to represent a final, small ($<1\%$) increment of the space-making portion of pluton emplacement.

THE STOPED BLOCKS

The stoped blocks (Fig. 5 a & b) are exposed on the glaciated floor of the Kaweah River canyon below Aster Lake. The outcrop comprises a sub-planar surface, dipping 15° to 20° westward, that is virtually 100% exposed. Vertical joint surfaces provide 3-dimensional exposure at many locations. The area was mapped on a 50 foot (15.2 m) grid constructed parallel to the ground surface using steel measuring tape, nylon rope, and Brunton compass.

The map area exposes three large blocks (30–140 m) and numerous smaller fragments of coarse-grained, biotite granite enveloped within medium-grained, hornblende–biotite granodiorite. Long axes of individual blocks and the overall block grouping trend west-northwest. Block contacts are knife-sharp and geometrically irregular, with long, gently curviplanar segments that meet at sharp corners. There is no macroscopic textural evidence for block assimilation by the granodiorite. The block shapes are apparently defined by sets of intersecting fractures, perhaps the fractures along which the

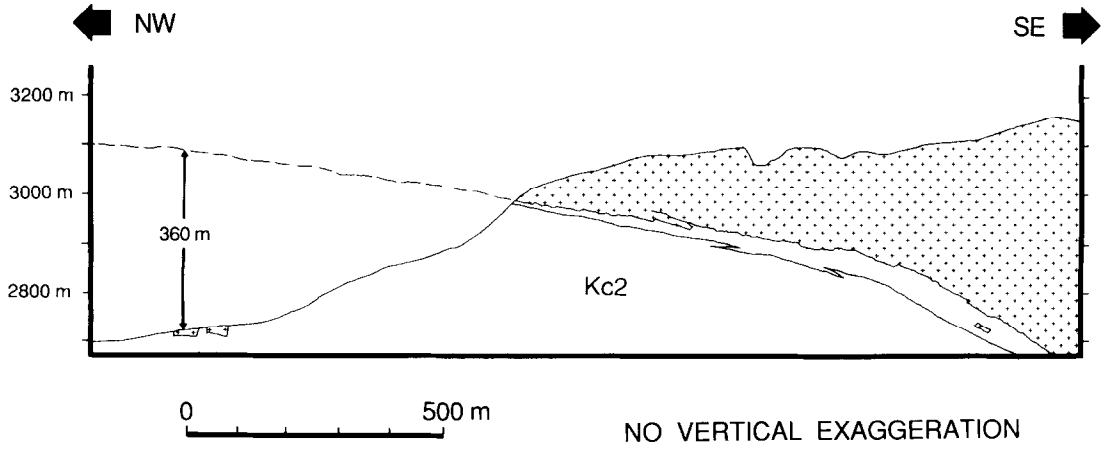

Fig. 4. Geological cross section showing location of stoped blocks with respect to projected position of the pluton roof contact. Map unit patterns are the same as in Fig. 2.

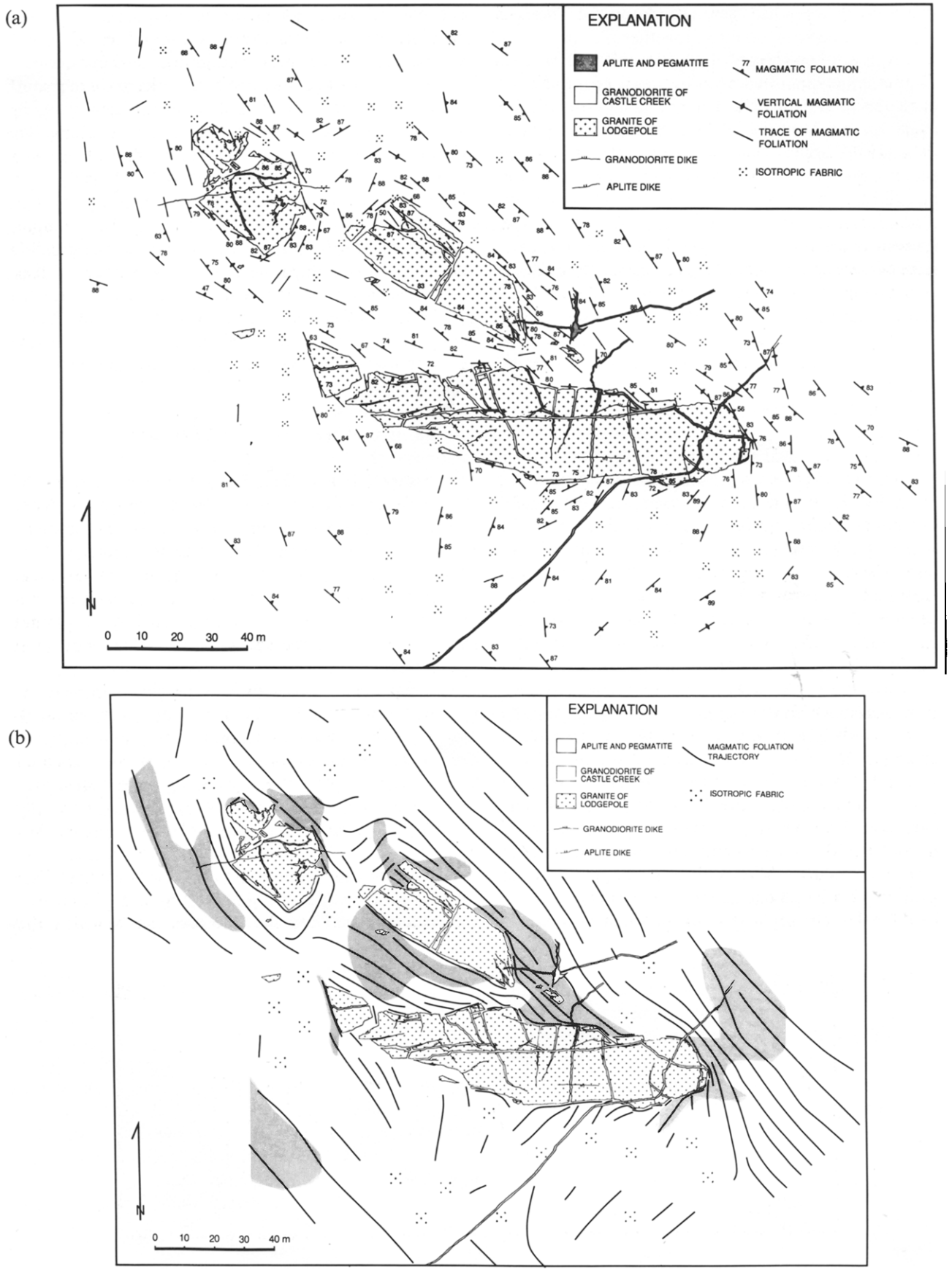

Fig. 5. (a) Geological map of stoped blocks showing magmatic foliations in granodiorite of Castle Creek. (b) Map showing trajectories of magmatic foliations in granodiorite of Castle Creek. Foliation dips are generally steeper than 75°. Darker shading shows areas of moderate qualitative foliation intensity, unshaded areas have weakly developed foliations, lighter shading indicates isotropic fabrics (see text).

blocks initially detached from the pluton roof. Some of the block shapes can be fitted together like pieces of a puzzle and were presumably once joined. For example, a small piece has separated by a few meters from the west end of the largest block, whereas the convex southern margin of the middle-sized block probably calved off from one of the two concave segments along the northern margin of the largest block.

Several generations of granodiorite, aplite, and banded aplite dikes cut the stoped blocks (Fig. 5a). Dike contacts generally dip-subvertically. Many of these dikes cut across the short dimension of the blocks, accommodating modest extension parallel to the length of the blocks. Because of continuity of the granodiorite dikes with the enveloping host and because of mutual cross-cutting relationships between granodiorite and aplite dikes, the dikes are interpreted to derive from the granodiorite of Castle Creek, and its late, highly evolved equivalents. Banded aplite material also occurs in a 5–30 cm-wide zone along some stoped block contacts (Fig. 6a). In many cases, these banded aplites intruded along block contacts at a relatively late time. Cross-cutting relations between compositional bands generally show younging of bands toward the stoped blocks, and some banded aplites are continuous with (fed by?) aplite dikes that cut across stoped block/granodiorite contacts. However, in other cases late movements of granodiorite magma may have truncated the banded aplites (Fig. 6b).

MAGMATIC FABRICS IN THE GRANODIORITE OF CASTLE CREEK

Mineral alignment foliations

The granodiorite of Castle Creek exhibits foliations defined by the preferred orientation of compositionally zoned, subhedral plagioclase, hornblende and biotite, set within a matrix of anhedral, equant quartz and potassium feldspar (Fig. 6d). Both framework and matrix grains show evidence for only minor intracrystalline plastic strain, as represented by weakly undulatory extinction in quartz. Grain contacts are commonly defined by crystal faces of the high-temperature phases, and show little evidence for grain boundary migration or recrystallization. The foliation is interpreted to have formed during magma crystallization, with sufficient melt present to permit rotation of the framework grains without accumulation of crystal–plastic strain — a 'pre-full crystallization fabric' in the terminology of Hutton (1988a), or 'magmatic foliation' in the terminology of Paterson *et al.* (1989). Magmatic fabrics in the granodiorite of Castle Creek are cut by, and therefore pre-date, late-plutonic aplite and pegmatite dikes.

Near the stoped blocks, magmatic foliations in the granodiorite of Castle Creek show a complex map pattern (Fig. 5a & b). Foliation dips are sub-vertical ($>70°$). The dominant feature of the map pattern is northwest-striking foliation that is parallel to foliations throughout this portion of the pluton (compare Figs 2 & 5b). Departures from northwest orientations occur in two areas, in a triangle-shaped region immediately south of the southern block, and also in and adjacent to the region between the two northern blocks. Foliations are parallel to most stoped block contacts within tens of centimeters from the contacts.

The most remarkable feature of the map pattern is the extreme narrowness of the zone of concordant, contact-parallel foliations in the granodiorite surrounding the blocks. Around 90% of the perimeter of the largest block, the width of this zone is ≤ 2 m and is commonly less than 1 m (Fig. 6a). At a few locations, weakly developed northwest-striking, steeply-dipping foliations in the granodiorite occur within a few centimeters of block contacts (Fig. 6c).

Qualitative estimates of fabric intensity in the granodiorite of Castle Creek were assigned to each of 280 stations in the mapped area, based on the following three-tier categorization (Fig. 5b): (1) apparently isotropic fabric; (2) weak mineral alignment (requiring close outcrop inspection to recognize); and (3) moderate mineral alignment (visible from a standing position). Relative to fabrics observed by the authors in other plutons, fabrics adjacent to the stoped blocks were nowhere strong. It is interesting to note that magmatic foliations tend to be weaker where they are oriented at a high angle to the dominant NW–SE km-scale fabric trend, such as in the area south of the southern block, or in the region between the two northern blocks. There is no simple relation between fabric intensity and distance from stoped block contacts; many contact segments are characterized by weak, or isotropic mineral fabrics.

Mineral alignment lineations

The preferred alignment of prismatic hornblende and plagioclase crystals define lineations in the granodiorite of Castle Creek. These lineations show microstructural features identical to the mineral foliations, and are also interpreted to be of primary magmatic origin (Hutton, 1988a; Blumenfeld and Bouchez, 1988; Paterson *et al.*, 1989). Unfortunately, a lack of exposures of foliation surfaces precludes observation of lineations at many localities in the map area and coverage is relatively poor. On the basis of limited observation, lineations appear to be only weakly developed. Seven out of twenty-one observations of foliation surfaces showed no discernible linear fabric. At some outcrops, lineation orientations vary by 45° within a few meters distance.

Linear magmatic fabrics near the stoped blocks mostly trend NW–SE (Figs 7 & 8). Lineation plunges are variable. Although lineations are steep adjacent to the east end of the southern block, lineations are shallow near the west end of the same block and near the northwestern-most block. Locally, at good exposures adjacent to the blocks, lineation is too weak to discern.

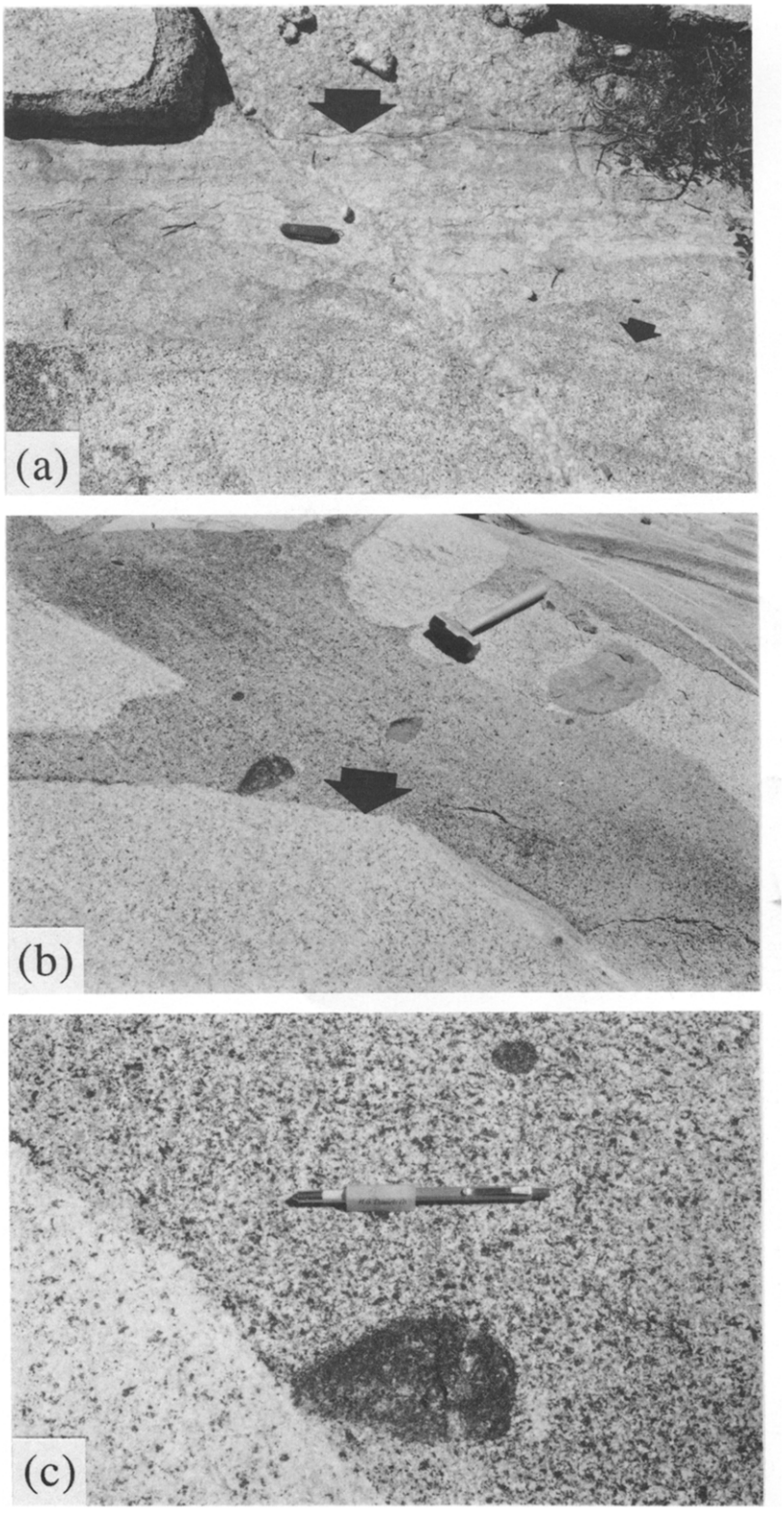

Fig. 6. Outcrop photos: (a) contact of coarse-grained granite stoped block crosses horizontally at top of photo (large arrow). Steep magmatic foliation in granodiorite (strike: 300°) lies parallel to faint compositional banding (small arrow) and makes angle of 30° with block contact. Note 25 cm-wide zone of banded aplite along block contact. Pocket knife is 9 cm long. (b) Aligned mafic enclaves in granodiorite of Castle Creek lie at 50° from stoped block contact (large arrow). Weak magmatic foliation (not visible in photo) is parallel to the enclaves. Obvious diagonal lineaments (upper L. to lower R.) are glacial striae. Note that banded aplites along the block contact appear to be truncated at the block corner to the right of the arrow. Hammer is 38 cm long. (c) Close-up of stoped block contact in Fig. 5(b). Pencil is parallel to trace of weak magmatic foliation visible in upper half of photo. Micrographs: (d) aligned mineral grains in granodiorite of Castle Creek trend horizontally across photo. a = amphibole; b = biotite; p = plagioclase; q = quartz. Base of photo is 14 mm. Crossed Nicols. (e) Contact between mafic enclave (left) and granodiorite of Castle Creek host (right) trends vertically across center of photo. Note alignment of mafic minerals in enclave parallel to contact. Base of photo is 9 mm. Plane polarized light. (*Continued overleaf.*)

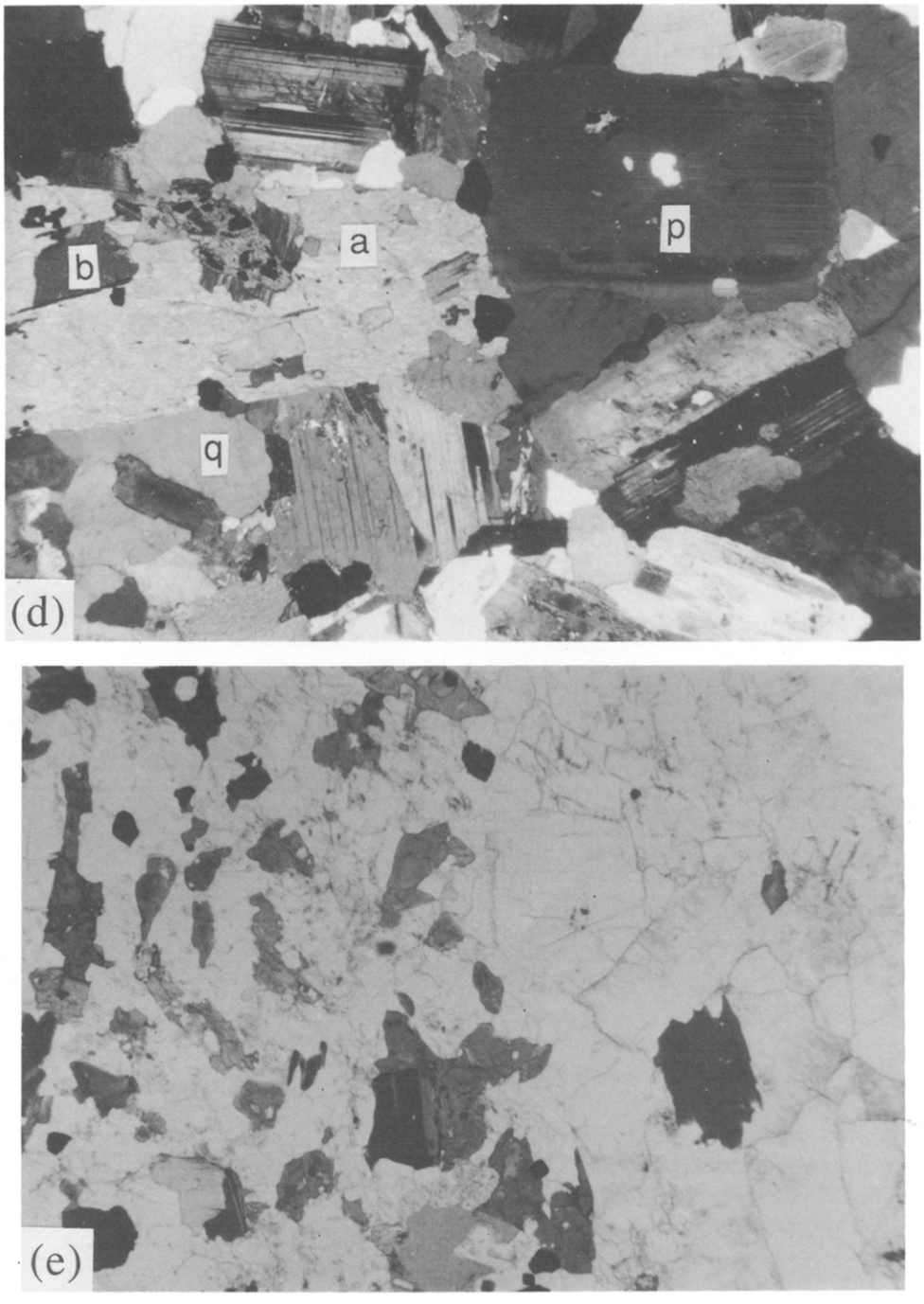

Fig. 6. (*Continued.*)

Farther from the stoped blocks (100–2000 m), magmatic lineations in the granodiorite of Castle Creek display dominantly NW–SE trends with shallow plunges (Fig. 8).

Fabrics defined by mafic enclaves

The granodiorite of Castle Creek contains abundant mafic enclaves, ranging from millimeters to a few tens of centimeters in size (Fig. 6b). Enclave modal compositions generally correspond to microdiorite, and except for proportional abundance and grain size, have mineralogy and texture similar to their granodiorite host. Many enclaves show textural features, such as lensoidal shape, drawn out wispy tails, and internal magmatic foliations (Fig. 6e) that have commonly been attributed to an origin by mingling of mafic and granodioritic magmas (Frost and Mahood, 1985; Vernon *et al.*, 1988; Didier and Barbarin, 1991). Measurements of the axial ratio and orientation of mafic enclaves yield a fabric ellipsoid. Although such mafic enclave fabrics have previously

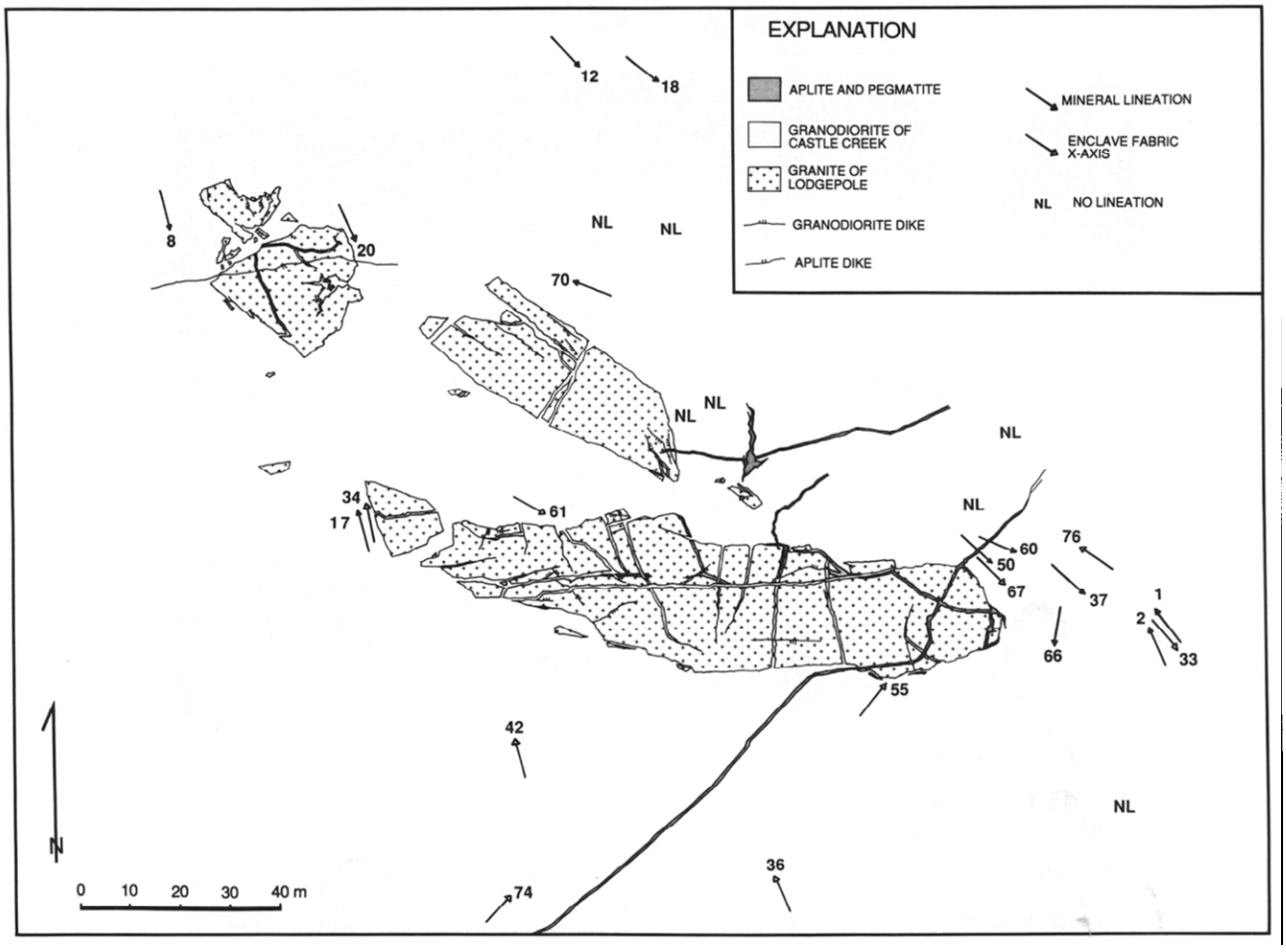

Fig. 7. Map showing orientations of hornblende lineation and enclave fabric *X*-axes in the granodiorite of Castle Creek.

been utilized as a measure of magmatic strain (Holder, 1979; Ramsay, 1989), controversy surrounds these interpretations (Cruden, 1990; Fernandez and Barbarin, 1991; Paterson and Fowler, 1993a; Paterson and Vernon, 1995). Here, we simply describe the anisotropic fabric defined by enclave shape and orientation, without reference to strain. Magmatic strain significance of the enclave fabrics is evaluated in the discussion section.

The Rf/Phi fabric analysis techniques used in this study (Shimamoto and Ikeda, 1976; Milton, 1980; Ramsay and

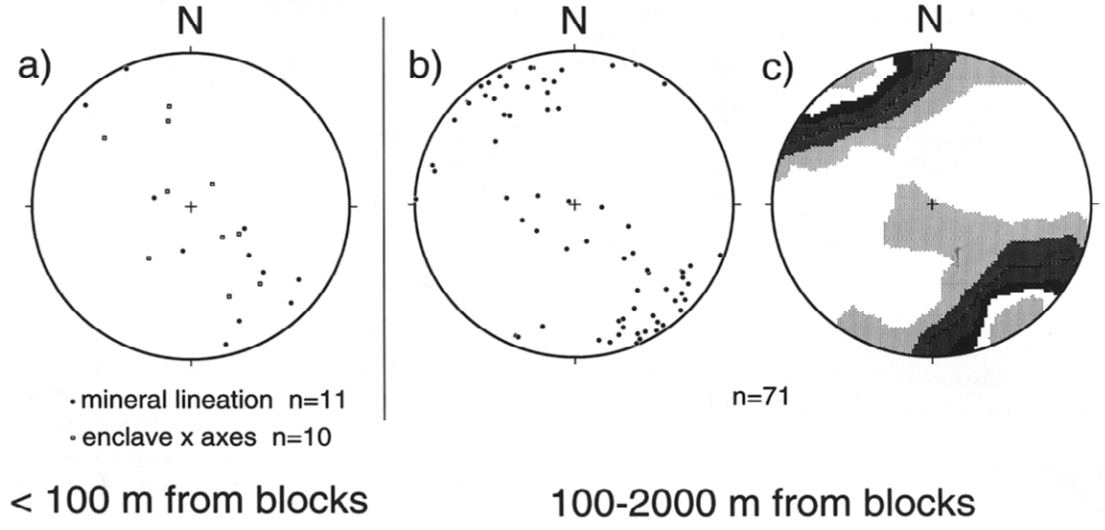

Fig. 8. Equal area stereographic projections showing: (a) granodiorite of Castle Creek mineral lineations (solid circles) and enclave fabric *x*-axes (open squares) from the area in Fig. 5; (b) granodiorite of Castle Creek mineral lineations from the area in Fig. 2 and > 100 m from stoped blocks; (c) Kamb contour plot of data in (b); contour interval = 2.0 sigma. Data in (b & c) from Fowler, 1996.

Table 1. (a) 3-D enclave fabric analysis results

Sta.	X	Y	Z	X/Y	X dir	Es	Lodes	n	Fol	Lin
1	2.14	1.96	1.00	319,88	67,134	0.591	0.7	48	325,82	NL
2	2.46	1.49	1.00	154,58	55,218	0.638	−0.108	68	233,63	NL
3	1.59	1.37	1.00	178,76	42,346	0.335	0.339	90	176,85	ND
4	1.69	1.42	1.00	339,76	34,348	0.376	0.335	75	342,82	18,345
5	1.67	1.54	1.00	104,82	61,120	0.319	0.668	59	282,75	NL
6	1.94	1.36	1.00	131,78	33,139	0.469	−0.074	88	142,80	1,322
7	1.74	1.53	1.00	152,83	76,304	0.409	0.538	90	333,73	ND
8	1.49	1.28	1.00	133,61	36,157	0.284	0.259	76	ND	ND
9	1.45	1.26	1.00	137,78	31,310	0.265	0.255	60	135,77	7,313
26	1.73	1.11	1.00	310,74	74,042	0.413	−0.630	76	322,84	ND

Table 1. (b) 2-D Enclave fabric data

Sta.	X/Y Ratio	X Trend	Mag Fol	n	Outcrop Surface
10	1.331	149	125,84	21	216,19
11	1.209	182	166	21	181,18
12	1.533	301	304,81	21	184,18
13	1.450	196	206,73	21	142,09
14	1.190	359	342,90	21	197,14
15	1.491	319	319,85	21	208,08
16	1.143	249	NF	21	185,18
17	1.327	035	024,84	21	163,15
18	1.137	063	NF	21	147,23
19	1.223	122	NF	21	147,16
20	1.229	201	203,82	21	169,16
21	1.530	323	334,74	21	172,19
22	1.643	297	333,68	21	154,18
23	1.451	320	311	21	165,15
24	1.500	086	078	21	172,16
25	1.863	329	322,72	21	163,20

(a) Sta. = station numbers shown in Fig. 9; X,Y,Z = lengths of principle axes; X/Y = orientation of ellipsoid X/Y plane; X dir = orientation of ellipsoid X-axis; Es = fabric intensity; Lodes = Lodes shape parameter; n = number of measurements; Fol and Lin = granodiorite magmatic foliation and lineation, respectively. NF = no discernible foliation in granodiorite.

Huber, 1983; Wheeler, 1986) are described in the Appendix. Overall, enclave fabrics near the stoped blocks are weak with somewhat variable ellipsoid shapes (Tables 1b & 2, Figs 9 & 10). Fabric ellipsoid intensities (Hossack, 1968) reach only $Es = 0.26$ to 0.64, with X/Z axial ratios generally $<2{:}1$. As given by the Lodes parameter (Hossack 1968), shapes of the fabric ellipsoids vary widely, from $\nu = 0.790$ (strongly oblate) to $\nu = -0.630$ (strongly prolate). Enclave fabrics are consistently oriented sub-parallel to mineral fabrics, with calculated ellipsoid X/Y planes generally $<15°$ from the foliation plane and ellipsoid X-axes $<25°$ from the lineation direction (Table 1).

Neither shape nor intensity of the enclave fabrics shows a strong relationship to distance from stoped block contacts. Inspection of Fig. 9 indicates that average enclave fabric intensities may show a slight increase within about 20 m of the blocks. However, weak enclave fabrics also occur immediately adjacent to, and oriented at high angles to stoped block contacts (Fig. 6b & c). Enclave X-axis plunges (Fig. 7), Lodes shape parameter and axial ratio of 2-D enclave fabrics (Fig. 9) show no relation to distances from block contacts. The population of enclave fabrics measured within 100 m of the stoped blocks is indistinguishable from enclave fabrics measured 100–2000 m from the blocks (Fig. 10).

DISCUSSION

Timing of fabric formation

Structural relations adjacent to the stoped blocks support three main conclusions regarding relative timing of fabric formation in the granodiorite of Castle Creek. First, there is little if any strain record for Newtonian Stokes flow related to sinking of the blocks. Second, km-scale fabric trends in the granodiorite of Castle Creek formed as or after the blocks reached their present position with respect to the enveloping magma. And third, since sinking and arrest of the blocks presumably represents the final stage of pluton emplacement, we argue that magmatic fabrics formed too late to record pluton space-making mechanisms.

Despite the large distance that the blocks are presumed to have sunk (several body-radius units), structures in the granodiorite of Castle Creek display little evidence for Stokes flow due to settling. For example, in an experiment by Cruden (1988), a passive marker grid of graphite particles was used to measure strains in a transparent Newtonian polymer during Stokes settling of a steel ball bearing. Sinking of the ball produced strong flattening strains (X/Z axial ratios $\geq 100{:}1$) in the polymer host adjacent to the ball's equatorial plane, with Z-axes of the strain ellipsoid oriented radially about the ball and with X-axes plunging sub-vertically. Pronounced strains were developed in the polymer host to a distance approximately equal to the radius of the ball. Contrary to model predictions, the region near the stoped blocks is dominated by km-scale foliation trends, which are only deflected into contact parallelism with the blocks within 2.0–0.02 m distance ($\approx$0.1–0.001 body radii). Available lineation data are not consistent with the strong vertical stretching predicted by the model. Additionally, the granodiorite fails to show the strong strain gradients and extreme strain intensities predicted by Newtonian Stokes-settling models; either such high strains have not occurred, or the granodiorite fabrics have failed to record

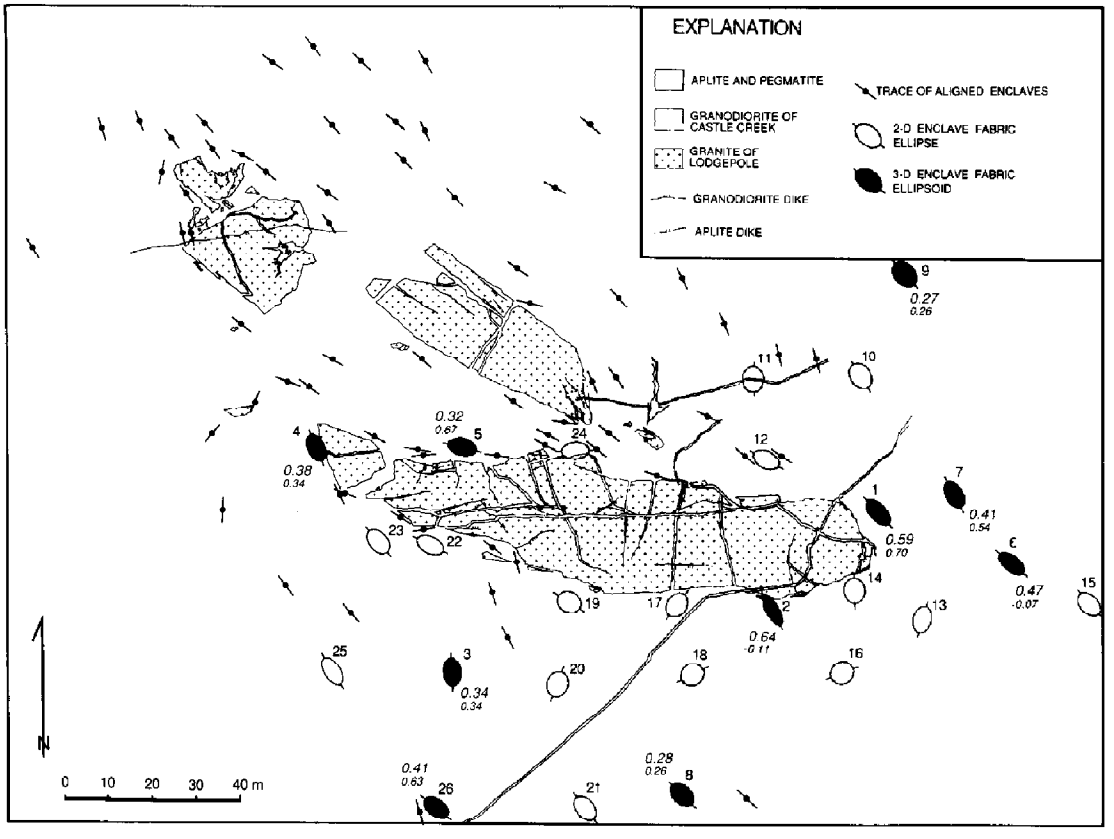

Fig. 9. Map showing fabrics defined by mafic enclaves in the granodiorite of Castle Creek as determined by Rf/Phi technique. Plain text numbers refer to station numbers in Table 1. Fabric ellipses on diagram show X/Z axial ratio and are oriented parallel to the strike of the ellipsoid X/Y plane. Large italic numbers give the fabric intensity parameter, Es; small italic numbers give the Lodes shape parameter, v. Orientation of enclave X-axes shown in Fig. 7. See text and Appendix for methods used and for definitions of fabric parameters.

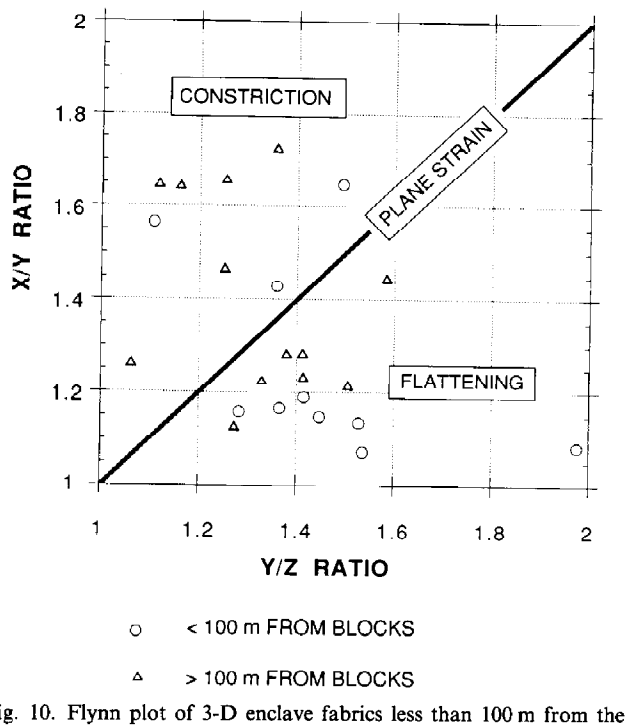

Fig. 10. Flynn plot of 3-D enclave fabrics less than 100 m from the stoped blocks (circles; $n = 10$) and 100–2000 m from the stoped blocks (triangles; $n = 13$). Note the near total overlap of the two populations. Enclave data 100–2000 m from blocks is from Fowler, 1996.

the strains. Qualitative mineral fabric intensities are moderate or weak and spatially heterogeneous. Mafic enclave fabric ellipsoid X/Z ratios reach only about 2:1, two orders of magnitude less than the $\geq$100:1 axial ratios predicted by the Stokes model (Cruden, 1988). On the one hand, the narrow width of the zone of concordant fabrics in the granodiorite of Castle Creek could potentially be explained by non-Newtonian flow of granodiorite magma. For instance, power-law flow would concentrate granodiorite deformation very near the blocks (e.g. $\approx$0.1 body radii, Weinberg and Podladchikov, 1994). On the other hand, concentration of deformation due to power-law flow would also tend to increase strain intensifies above already large Newtonian model strains. Weak mineral and enclave fabric intensities observed near the blocks are not compatible with the strain concentrations predicted by power-law flow.

The following structural relations strongly suggest that the stoped blocks and granodiorite magma experienced mutual NE-directed shortening and NW-directed extension during formation of km-scale fabric trends in the granodiorite of Castle Creek: (1) individual blocks and the grouping as a whole are elongate to the northwest, suggesting block rotation into the magmatic foliation plane; (2) the several blocks probably represent fragments of a once larger mass that has been pulled apart

parallel to the foliation plane; (3) granodiorite dikes within individual blocks are compatible with extension parallel to the foliation plane; (4) the extension direction suggested by the blocks is sub-parallel to km-scale, NW-SE trending, shallowly plunging magmatic lineation trends in the pluton (Fig. 8); (5) local deflection of magmatic foliation trajectories suggests flow of granodiorite into regions between the separated blocks; (6) relatively strong granodiorite fabrics along northwest-striking block contacts (Fig. 5b) may record the stress/strain concentrations that drove block rotation; (7) weak granodiorite fabrics between the blocks and south of the largest block appear to be strain shadows or pressure shadows in regions shielded by the blocks.

The above structural relations favor the following two interpretations concerning relative timing of stope block sinking and formation of km-scale magmatic fabric trends in the granodiorite of Castle Creek: (1) km-scale fabric trends entirely post-date sinking and arrest of the stoped blocks; in this case, local deflection of fabric trends would reflect stress and strain rotation near block contacts during km-scale NE-shortening and NW-extension; or (2) km-scale fabrics formed during sinking of the blocks; in this case, local deflection of fabric trends would reflect block sinking and rotation during the formation of NW-trending fabric. In our view, fabrics related to block sinking are so poorly developed that we prefer the former interpretation. Whichever of the above scenarios is correct, continuing formation of km-scale fabric trends in the granodiorite of Castle Creek is temporally linked to sinking of the stoped blocks. We argue that block sinking cannot be a later event, superimposed upon pre-existing km-scale fabric trends.

Preserved stoped blocks make up $< 1\%$ of the outcrop area of the granodiorite of Castle Creek, and are interpreted above to represent a final, tiny increment of the space-making process. If this interpretation is correct, then magmatic fabrics in the granodiorite of Castle Creek continued to form after most or all of the space for pluton emplacement had already been created, and thus, formed too late to record emplacement mechanisms.

Magma strain memory

Magmatic fabrics in the granodiorite of Castle Creek apparently fail to record the mechanism by which large granite xenoliths were engulfed and transported hundreds of meters, implying a significant loss of strain memory. The deformation of partially molten rocks constitutes a recognized, fundamental problem for strain analysis (Fernandez, 1988; Launeau *et al.*, 1990; Borradaile, 1988). For example, Means and Park (1993) and Park and Means (in press) observed that fabrics formed in an experimental non-silicate crystal-melt mush showed similar geometries across a wide range of deformation states. Furthermore, if sufficient melt is present to allow grain rotation, it seems reasonable that early mineral alignment fabrics could potentially be altered or re-set during subsequent magmatic-state deformation. Thus, determination of total magma strains from magmatic fabrics may be impossible. The implications for interpretation of fabric patterns in plutons are obvious and have been recognized by many previous workers (Pitcher, 1993). Virtually all strain record for magma ascent and emplacement may be lost during small strains caused by regional tectonics, magma surges, or other late-stage processes.

Near the stoped blocks, mafic enclave fabric ellipsoid X/Z ratios reach only 2:1, suggesting that the enclaves do not record magmatic strains completely. A possible explanation for this lack of enclave deformation relates to rheological changes driven by magma crystallization (Arzi, 1978; van der Molen and Paterson, 1979; Laporte, 1994). Fernandez and Barbarin (1991) outline a hypothetical enclave strain history based on expected variations in magma rheology during crystallization of mingled mafic and felsic magmas. These authors argue that at high temperatures, the melt fraction of both mafic enclaves and host felsic magma will be large, the viscosity of mafic enclaves will be less than that of the felsic host magma, and the enclaves should readily deform. At some point during cooling, a rheological reversal comes, in which the enclaves become significantly more crystalline, and thus, significantly stronger than the felsic host magma. At this point, mafic enclaves should behave as rigid particles (Cruden, 1990; Williams and Tobisch, 1994). This rheological scenario poses two chief consequences for strain analysis. First, mafic enclaves measured in outcrop almost certainly inherit a shape anisotropy resulting from early, high-temperature strain. This shape anisotropy may represent only brief, localized deformation events, such as the disaggregation and quenching of a syn-plutonic mafic dike (Williams and Tobisch, 1994), and may not reflect the overall strain history of the host magma. Second, for a significant portion of the crystallization history, enclaves are expected to behave as rigid particles, unable to record bulk strain of the host magma (Cruden, 1990; Fernandez and Barbarin, 1991).

Implications for interpreting causes of magmatic fabrics

Magmatic fabrics in plutons can form extremely late during emplacement and image a strain history that can be decoupled from strains in the surrounding host rocks. Consequently, magmatic fabric map patterns generally cannot be interpreted in terms of pluton emplacement, regional tectonics, or internal magma chamber processes without additional structural information.

We describe a single spectacular example of late-formed magmatic fabrics, but many other examples exist. Magmatic foliations in the early, finer-grained facies of the granodiorite of Castle Creek follow km-scale orientation trends to within 1–2 m of the locally-preserved tops, sides and bottoms of large stoped blocks before deflecting into contact parallelism (Fig. 11).

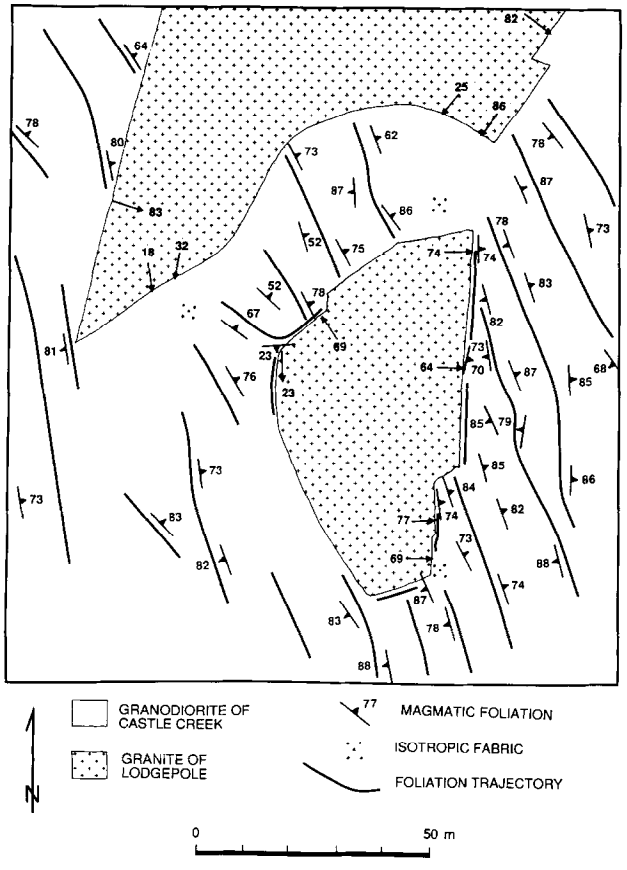

Fig. 11. Geologic map of stoped granite of Lodgepole blocks contained within the granodiorite of Castle Creek 1. North-northwest strike and steep dip of magmatic foliations in the map area reflect km-scale trends in the granodiorite of Castle Creek. Foliations only deflect into concordance with the stoped blocks within a few meters of the contact.

Evidence for sinking of the blocks has been destroyed. We have also observed undeflected and/or weak magmatic fabrics around stoped blocks in the Mt Powell batholith, Montana, the Mt Stuart batholith, Washington, the Hall Canyon pluton, California, and the Chita pluton, San Juan Province, Argentina. An additional body of published field data corroborates the late formation of magmatic fabrics in plutons. As noted by Buddington (1959), Pitcher (1993) and Paterson and Vernon (1995) among others, magmatic foliations commonly cross-cut, and must therefore post-date, contacts between compositional or textural facies in zoned plutons (Pitcher and Berger, 1972; Guillet *et al.*, 1985; Bateman, 1992).

Comparison of structures within plutons and their host rocks indicates that in some cases, pluton and host strains are at least partially decoupled. In the Mitchell Intrusive Suite, both mineral alignment and enclave fabrics are parallel to steep walls and shallow roof contacts, suggesting the possibility of forcible intrusion (Figs 2 & 3). However, the host rocks show no evidence for forcible emplacement. On the contrary, pluton contacts are brittle fractures that truncate structures and fabrics in the otherwise undeformed granite of Lodgepole (Fowler, 1994a, 1996). There are other examples of contact-parallel foliations occurring within discordant plutons, suggesting that at least partial decoupling of pluton and host rock strain is probably common (references in Paterson and Vernon, 1995). The mechanical basis for both contact-parallel structures and strain decoupling presumably depends upon the competency contrast between magma and solid host rock; during deformation, strain is concentrated within the weaker material near the contact with the stronger one. These mechanical conditions are particularly likely to occur in the brittle upper crust.

Because of late timing of formation, poor strain memory, and decoupling of pluton and host rock strains, magmatic fabrics cannot constrain the quantitative importance of pluton emplacement mechanisms. For example, concentric, contact-parallel magmatic foliations do not require ballooning emplacement (Schmeling *et al.*, 1988; Paterson and Vernon, 1995), nor do enclave fabrics necessarily record magma chamber expansion. Commonly, enclave fabric intensities in plutons are different from strain intensities in the adjacent country rocks (Fowler and Paterson, 1991, references in Paterson and Fowler, 1993a), an observation consistent with strain decoupling. Alternatively, spatial and kinematic links between magmatic fabrics and regional faults have been used to argue that local, fault-controlled dilation is an important space-making mechanism for plutons (Guineberteau *et al.*, 1987; Hutton, 1988b). Although such evidence can demonstrate synchronous regional faulting and plutonism, it cannot constrain the magnitude of fault-controlled dilation, or even determine whether or not dilation has actually occurred. Thus, the quantitative importance of emplacement mechanisms can only be estimated using strain and displacement fields in the host rocks. Estimates of the magnitude of diapirism and ballooning must come from quantitative structural reconstructions of contact aureoles (Sanderson and Meneilly, 1981; Bateman, 1985; Brun *et al.*, 1990; England, 1992; Paterson and Fowler, 1993a; Fowler, 1994b); estimates of fault-controlled dilation must come from offsets and deflections of geological markers (Woodcock and Underhill, 1987; Paterson and Fowler, 1993b).

Since magmatic fabrics may largely form after the space-making phase of emplacement is over, it seems likely that they more commonly image strains caused by regional tectonic deformation and/or by late internal magma chamber processes. Kinematic and temporal links between pluton and host-rock structures can establish the role of tectonic strains in the formation of magmatic fabrics. This approach has been particularly successful for plutons emplaced near or into active shear zones, where in many cases, a geometrically coherent progression of magmatic to solid-state pluton fabrics has been documented (Guineberteau *et al.*, 1987; Blumenfeld and Bouchez, 1988; Hutton, 1988b; Archanjo *et al.*, 1994; Nedelec *et al.*, 1994; Vauchez *et al.*, 1995). By a similar argument, NW-striking magmatic foliations and shallow

NW-trending lineations in the Mitchell Intrusive Suite may image weak, regional tectonic strains during pluton crystallization (Fowler, 1996). Evidence for regional NE-directed shortening during right-lateral transpression is widespread in 92–78 Ma plutons in the central Sierra Nevada batholith (Busby-Spera and Saleeby, 1990; Bateman, 1992; Tikoff and Teyssier, 1994b; Tobisch *et al.*, 1995) and is compatible with plate motion reconstructions (Engebretson *et al.*, 1985).

A wide variety of internal magma chamber processes could produce observed fabric patterns in plutons, including: (1) pulsed intrusion; (2) magma surges; (3) eruption of material from the chamber; (4) thermal/compositional density instabilities arising from crystallization. Because all of these can be relatively late processes, they have a high potential for structural preservation. Evidence for pulsed intrusion of magma batches is common, before, during and after crystallization of earlier magma pulses (Pitcher, 1993). Pulsed magma intrusion is predicted by diapir models, which suggest that passage of early magma provides a thermally-softened conduit for subsequent magmas (Marsh, 1982), and also by models which call on magma ascent through dikes (Clemens and Mawer, 1992). Pulsed intrusion does not necessarily imply growth of the magma chamber. Space for subsequent magma pulses can potentially be made by a combination of volume contraction during cooling (John and Blundy, 1993), downward return flow (Paterson and Vernon, 1995), or volcanic venting of older magma. Alternatively, crystallization along magma chamber roofs and walls should lead to thermal/compositional density instabilities that could drive magma surges; the molten pluton core may intrude its own solidifying rind. Relatively small magma displacements, due to any of the above causes, can produce typical magmatic fabric patterns. According to Cruden (1990), internal circulation of only 0.2 overturns should produce fabric intensities of the same order as typically observed in plutons.

Of the potential causes for magmatic fabrics, internal magma chamber processes are the most difficult to evaluate. Since internal processes inherently involve decoupling of pluton and host rock strains, they can only be fully demonstrated in cases where emplacement and tectonic processes have been ruled out. In the worst cases, the causes of magmatic fabrics cannot be uniquely determined. This is unfortunate; we suspect that in many instances where magmatic fabrics have been attributed to ascent or emplacement mechanisms (e.g. magma feeder zones, direction/magnitude of asymmetrical ballooning, direction of tectonic opening), they could just as plausibly represent late magma pulses or surges.

CONCLUSIONS

Stoped granite blocks in the granodiorite of Castle Creek currently rest approximately 360 m below the pluton roof contact from which they presumably detached. Detachment and sinking of the blocks is interpreted to represent the final, tiny increment of the space-making portion of pluton emplacement. Surprisingly, magmatic fabrics in granodiorite surrounding the stoped blocks show little or no evidence for Stokes flow related to block sinking. Instead, fabrics in the granodiorite follow km-scale orientation trends to within 1–2 m of the blocks before deflecting into concordance with block contacts. Map relations suggest that the stoped blocks and enveloping magma experienced mutual NE-directed shortening and NW-directed extension; brittle fragmentation and inferred rotations of the blocks indicate shortening and extension directions consistent with magmatic fabric trends in the pluton. From these relations, we argue that magmatic fabrics in the granodiorite of Castle Creek continued to form after sinking of the blocks, during or after the fast, tiny increment of the space-making phase of pluton emplacement. Parallelism of these magmatic fabrics with regional dextral and reverse shear zones suggests that they resulted from weak tectonic strains during magma crystallization.

These observations and other published data suggest that magmatic fabrics may commonly form too late to record space-making mechanisms, that magmatic fabrics have poor strain memory, and that pluton and host-rock strains can be mechanically decoupled, especially in the brittle upper crust. Consequently, magmatic fabric map patterns cannot be interpreted in terms of pluton emplacement mechanisms, regional tectonics, or internal magma chamber processes without additional structural information. In particular, the quantitative importance of pluton emplacement mechanisms can only be evaluated using strain and displacement fields from the host rocks.

Acknowledgements—This work was supported by NSF grant No. EAR-9304058. Fowler received additional support from Graduate Merit and Doctoral Dissertation Fellowships from the University of Southern California. We also thank Drs A. R. Cruden, B. K. Davis and B. Ildefonse for thoughtful and constructive reviews.

REFERENCES

Ague, J. J. and Brimhall, G. H. (1988) Magmatic arc asymmetry and distribution of anomalous plutonic belts in the batholiths of California: effects of assimilation, crustal thickness, and depth of crystallization. *Bulletin of the geological Society, America* **100**, 912–927.

Archanjo, C. J., Bouchez, J.-L., Corsini, M. and Vauchez, A. (1994) The Pombal granite pluton: magnetic fabric, emplacement and relationships with the Brasiliano strike-slip setting of NE Brazil (Paraiba State). *Journal of Structural Geology* **16**, 323–335.

Arzi, A. A. (1978) Critical phenomena in the rheology of partially melted rocks. *Tectonophysics* **44**, 173–184.

Balk, R. (1937) Structural behavior of igneous rocks. *Memoirs of the Geological Society, America* **5**.

Barriere, M. (1981) On curved laminae, graded layers, convection currents and dynamic crystal sorting in the Ploumanac'h (Brittany) subalkaline granite. *Contributions to Minereralogy & Petrology* **77**, 214–224.

Bateman, R. (1985) Aureole deformation by flattening around a diapir during in situ ballooning: the Cannibal Creek granite. *Journal of Geology* **93**, 293–310.

Bateman, P. C. (1992) Plutonism in the central part of the Sierra Nevada batholith. *U.S. geological Survey Professional Paper* 1483.

Bergantz, G. W. Physical and chemical characterization of plutons. In *Contact Metamorphism*, ed. D. M. Kerrick, Vol. **26**, pp. 13–42. *Mineral Society, America Reviews in Mineralogy.*

Blumenfeld, P. and Bouchez, J.-L. (1988) Shear criteria in granite and migmatite deformed in the magmatic and solid states. *Journal of Structural Geology* **10**, 361–372.

Borradaile, G. J. (1988) Magnetic susceptibility, petrofabrics and strain. *Tectonophysics* **156**, 1–20.

Bouchez, J.-L. and Gleizes, G. (1995) Two-stage deformation of the Mont-Louis-Andorra granite pluton (Variscan Pyrenees) inferred from magnetic susceptibility anisotropy. *Journal of the Geological Society, London* **152**, 669–679.

Brun, J. P., Gapais, D., Cogne, J. P., Ledru, D. and Vigneresse, J. L. (1990) The Flamanville granite (NW France): an unequivocal example of a syntectonically expanding pluton. *Journal of Geology* **25**, 271–286.

Buddington, A. F. (1959) Granite emplacement with special reference to North America. *Bulletin of the geological Society, America* **70**, 671–747.

Busby-Spera, C. J. (1983) Paleogeographic reconstruction of a submarine volcanic center: geochronology, volcanology, and sedimentology of the Mineral King roof pendant, Sierra Nevada, California. Unpublished Ph.D. Thesis, Princeton University, Princeton, New Jersey, U.S.A.

Busby-Spera, C. J. and Saleeby, J. B. (1990) Intra-arc strike-slip fault exposed at batholithic levels in the southern Sierra Nevada, California. *Geology* **18**, 255–259.

Chen, J. H. and Moore, J. G. (1982) Uranium–lead isotopic ages from the Sierra Nevada batholith, California. *Journal of geophysical Research* **87**, 4761–4784.

Clemens, J. D. and Mawer, C. K. (1992) Granitic magma transport by fracture propagation. *Tectonophysics* **204**, 339–360.

Cloos, H. (1925) Einfurhrung in die tectonische Behandlung magmatischer Erscheinungen, pt 1. Das Riesengebirge in Shlesien. Gebr., Borntraeger. Berlin.

Cruden, A. R. (1988) Deformation around a rising diapir modeled by creeping flow past a sphere. *Tectonics* **7**, 1091–1101.

Cruden, A. R. (1990) Flow and fabric development during diapiric rise of magma. *Journal of Geology* **98**, 681–698.

Dell'Angelo, L. N., Tullis, J. and Yund, R. A. (1987) Transition from dislocation creep to melt-enhanced diffusion creep in fine-grained granitic aggregates. *Tectonophysics* **139**, 325–332.

Didier, J. and Barbarin, R. (eds) (1991) *Enclaves and Granite Petrology.* Elsevier, Oxford.

Dixon, J. M. (1975) Finite strain and progressive deformation in models of diapiric structures. *Tectonophysics* **28**, 89–124.

Engebretson, D. C., Cox, A. and Gordon, R. G. (1985) Relative motions between oceanic and continental plates in the Pacific basin. Special Paper of the geological Society, America **206**.

England, R. W. (1992) The genesis, ascent and emplacement of the northern Arran granite, Scotland: implications for granitic diapirism. *Bulletin of the Geological Society, America* **104**, 606–614.

Fernandez, A. (1988) Strain analysis from shape preferred orientation in magmatic rocks. In *Geological Kinematics and Dynamics* (in Honor of the 70th Birthday of Hans Ramberg) *Bulletin of the geological Institution, University of Uppsala* **14**, 61–67.

Fernandez, A. and Barbarin, B. (1991) Relative rheology of coeval mafic and felsic magmas: nature of resulting interaction processes. Shape and mineral fabrics of mafic microgranular enclaves. In *Enclaves and Granite Petrology*, eds J. Didier and B. Barbarin, pp. 116–128. Elsevier, Oxford.

Fowler, T. K., Jr (1994a) Granitoid emplacement into older plutonic host-rocks. *Abstracts Programs of the Geological Society, America* **26**, A-134.

Fowler, T. K., Jr (1994b) Using geologic maps to constrain pluton emplacement mechanisms. *Abstracts Programs of the Geological Society, America* **26**.

Fowler, T. K., Jr (1996) Pluton roofs: testing pluton emplacement hypotheses. Unpublished Ph.D. Thesis, University of Southern California, Los Angeles, California, U.S.A.

Fowler, T. K., Jr and Paterson, S. R. (1991) On the role of ductile wall rock deformation during pluton emplacement: constraints from quantitative strain analysis. *Abstracts Programs of the geological Society, America* **23**.

Frost, T. P. and Mahood, G. A. (1987) Field, chemical and physical constraints on mafic–felsic magma interaction in the Lamarck granodiorite, Sierra Nevada, California. *Bulletin of the Geological Society, America* **99**, 272–291.

Guillet, P., Bouchez, J. L. and Vigneresse, J. L. (1985) Le complexe granitique de Plouaret (Bretagne): Mise en evidence structural et gravametrique de diapirs emboites. *Bulletin of the Geological Societyy, France* **8**, 503–513.

Guineberteau, B., Bouchez, J. L. and Vigneresse, J. L. (1987) The Mortagne granite pluton (France) emplaced by pull-apart along a shear zone: structural and gravimetric arguments and regional implications. *Bulletin of the geological Society, America* **99**, 763–770.

Holder, M. T. (1979) An emplacement mechanism for post-tectonic granites and its implications for their geochemical features. In *Origin of Granite Batholiths: Geochemical Evidence*, eds M. P. Atherton and J. Tarney, pp. 116–128. Shiva Publ., Kent, U.K.

Hossack, J. R. (1968) Pebble deformation and thrusting in the Bygdin area (S. Norway). *Tectonophysics* **5**, 315–339.

Hutton, D. W. H. (1988a) Granite emplacement mechanisms and tectonic controls: inferences from deformation studies. *Transactions of the Royal Society, Edinburgh* **79**, 245–255.

Hutton, D. W. H. (1988b) Igneous emplacement in a shear zone termination: the biotite granite at Strontian, Scotland. *Bulletin of the Geological Society, America* **100**, 1392–1399.

Ildefonse, B., Launeau, P., Bouchez, J.-L. and Fernandez, A. (1992) Effect of mechanical interactions on the development of shape preferred orientations: a two-dimensional experimental approach. *Journal of Structural Geology* **14**, 73–83.

John, B. E. and Blundy, J. D. (1993) Emplacement-related deformation of granitoid magmas, southern Adamello massif, Italy. *Bulletin of the Geological Society, America* **105**, 1517–1541.

Laporte, D. (1994) Wetting behavior of partial melts during crustal anatexis: the distribution of hydrous silicic melts in polycrystalline aggregates of quartz. *Contributions to Mineral Petrology* **116**, 486–499.

Launeau, P., Bouchez, J.-L. and Benn, K. (1990) Shape preferred orientation of object populations: automatic analysis of digitized images. *Tectonophysics* **180**, 201–211.

Marre, J. (1986) *The Structural Analysis of Granitic Rocks.* Elsevier, Oxford.

Marsh, B. D. (1982) On the mechanics of diapirism, stoping and zone melting. *American Journal of Science* **282**, 808–855.

Marsh, B. D. (1989) Magma chambers. *Annual Reviews of Earth and Planetary Science* **17**, 439–474.

Means, W. D. and Park, Y. (1993) Analog experiments suggest need for caution in interpreting strains and flow processes from fabrics in plutons. *Abstracts Programs of the Geological Society, America* **25**, A305.

Milton, N. J. (1980) Determination of the strain ellipsoid from measurements on any three sections. *Tectonophysics* **64**, T19–T27.

Moore J. G. and Sisson, T. W. (1987) Geologic Map of the Triple Divide Peak Quadrangle, Tulare County, *California. U.S. geological Summary* Map GQ-1936, scale 1:62,500.

Nedelec, A., Paquette, J.-L., Bouchez, J.-L., Olivier, P. and Ralison, B. (1994) Stratoid granites of Madagascar: structure and position in the Panafrican orogeny. *Geodynamic Acta* **7**, 48–56.

Nicolas, A., Freydier, C. I., Godard, M. and Vauchez, A. (1993) Magma chambers at oceanic ridges: how large? *Geology* **21**, 53–56.

Park, Y. and Means, W. D. (in press). Crystal rotation and growth during grain flow in a deforming crystal mush. *Journal of Structural Geology.*

Paterson, S. R. and Fowler, T. K. (1993a) Re-examining pluton emplacement processes. *Journal of Structural Geology* **15**, 191–206.

Paterson, S. R. and Fowler, T. K. (1993b) Extensional pluton emplacement models: do they work for large plutonic complexes? *Geology* **21**, 781–784.

Paterson, S. R. and Vernon, R. H. (1995) Bursting the bubble on ballooning plutons: a return to emplacement of nested diapirs. *Bulletin of the Geological Society, America* **107**, 1356–1380.

Paterson, S. R., Vernon, R. H. and Tobisch, O. T. (1989) A review of criteria for the identification of magmatic and tectonic foliations in granitoids. *Journal of Structural Geology* **11**, 349–363.

Phillips, W. J., Fuge, R. and Phillips, N. (1981) Convection and crystallization in the Criffel-Dalbeattie granodiorite complex. *Quaternary Journal of the Geological Society, London* **138**, 221–239.

Pitcher, W. S. (1993) *The Nature and Origin of Granite.* Blackie Academic and Professional, London.

Pitcher, W. S. and Berger, A. R. (1972) *The Geology of Donegal: A Study of Granite Emplacement and Unroofing*. Wiley-Interscience, New York.

Ramberg, H. (1981) *Gravity, Deformation and the Earth's Crust: in Theory, Experiments and Geological Application*, Academic Press, New York.

Ramsay, J. G. (1989) Emplacement kinematics of a granitic diapir: the Chinamora batholith. *Journal of Structural Geology* **11**, 191–210.

Ramsay, J. G. and Huber, M. I. (1983) *The Techniques of Modern Structural Geology*. Volume 1: *Strain Analysis*. Academic Press, London.

Rushmer, T. (1995) Application of rock deformation experiments to melt segregation in the lower crust. In *The Origin of Granites and Related Rocks*, eds M. Brown and M. Piccoli. *U.S. geological Survey Circular* **1129**, 130–131.

Sanderson, D. J. and Meneilly, A. W. (1981) Analysis of three-dimensional strain modified uniform distributions: andalusite fabrics from a granite aureole. *Journal of Structural Geology* **3**, 109–116.

Schmeling, H., Cruden, A. R. and Marquart, G. (1988) Deformation in and around a fluid sphere moving through a viscous medium: implications for diapiric ascent. *Tectonophysics* **149**, 17–34.

Shimamoto, I. and Ikeda, Y. (1976) A simple algebraic method for strain estimation from deformed ellipsoidal objects. 1: Basic theory. *Tectonophysics* **36**, 315–337.

Sisson, T. M and Moore, J. G. (1984) Geology of the Giant Forest–Lodgepole area, Sequoia National Park, California. *U.S. geological Survey Open File Report* 84–254.

Stephens, W. E. (1992) Spatial, compositional, and rheological constraints on the origin of zoning in the Criffell pluton, Scotland. *Transactions of the Royal Society, Edinburgh* **83**, 191–199.

Tikoff, B. and Teyssier, C. (1994a) Strain and fabric analysis based on porphyroclast interaction. *Journal of Structural Geology* **16**, 477–491.

Tikoff, B. and Teyssier, C. (1994b) Dextral shearing in the east-central Sierra Nevada magmatic arc: implications for Late Cretaceous tectonics and passive emplacement of granite. *Abstracts Programs of the Geological Society, America* **23**, A176.

Tobisch, O. T., Saleeby, J. B., Renne, P. R., McNulty, B. and Tong, W. (1995) Variations in deformation fields during development of a large-volume magmatic arc, central Sierra Nevada, California. *Bulletin of the Geological Society, America* **107**, 148–166.

van der Molen, I. and Paterson, M. S. (1979) Experimental deformation of partially melted granite. *Contributions to Mineral Petrology* **70**, 299–318.

Vauchez, A., Neves, S., Caby, R., Corsini, M., Egydio-Silva, M., Arthaud, M. and Amaro, V. (1995) The Borborema shear zone system, NE Brazil. *Journal of South American Earth Science* **8**, 247–266.

Vernon, R. H., Etheridge, M. A. and Wall, V. J. (1988) Shape and microstructure of microgranitoid enclaves, indicators of magma mingling and flow. *Lithos* **22**, 1–11.

Weinberg, R. F. and Podladchikov, Y. (1994) Diapiric ascent of magmas through power-law crust and mantle. *Journal of geophysical Research* **99**, 9543–9560.

Wheeler, J. (1986) Strain analysis in rocks with pre-tectonic fabrics. *Journal of Structural Geology* **7**, 667–682.

Williams, Q. and Tobisch, O. T. (1994) Microgranitic enclave shapes and magmatic strain histories: constraints from drop deformation theory. *Journal of geophysical Research* **99**, 24359–24368.

Woodcock, N. H. and Underhill, J. R. (1987) Emplacement-related fault patterns around the northern Arran granite, Arran, Scotland. *Bulletin of the Geological society, America* **98**, 515–527.

APPENDIX

Mafic enclave fabrics in the granodiorite of Castle Creek were measured by three methods. First, the average long-axis trace of groups of well-aligned enclaves was estimated on shallowly-dipping outcrop surfaces using a compass. Second, at 16 map stations, 2-D enclave fabrics were determined by Rf/Phi technique (Ramsay & Huber 1983). For each 2-D analysis, 21 measurements of enclave axial ratio and long-axis orientation were made on a shallowly-dipping outcrop surface. From these data, a 2-D fabric ellipse was calculated by the matrix method of Shimamoto & Ikeda (1976). Because magmatic fabrics in the mapped area dip steeply, the 2-D data reliably portray the strike of enclave 3-D planar fabrics, with the calculated 2-D axial ratio values falling between the X/Z and Y/Z ratios of the true 3-D ellipsoid (Ramsay 1989). Third, 3-D enclave fabric ellipsoids were determined at 10 map stations. For the 3-D analyses, an average of 24 (minimum 8; maximum 30) enclaves were measured on each of three joint surfaces oriented at high angles to one another (total n, each station = 48 to 90). These data were used to calculate 2-D fabric ellipses for each joint surface. The three 2-D fabric ellipses from each station were then combined into a 3-D fabric ellipsoid with the program '2D > 3D Strain' by K. Kanagawa, which utilizes the tensor algebraic method of Wheeler (1986) and the method of Milton (1980) for calculating an ellipsoid from data on three non-orthogonal surfaces.

The results of the fabric analyses are presented in Figs 9 & 10 and Table 1 as ratios and orientations of the principle axes, and intensity and shape of the fabric ellipsoid. Fabric intensity was calculated according the formula of Hossack (1968):

$$E_S = \frac{1}{3}[(e_1 - e_2)^2 + (e_2 - e_3)^2 + (e_3 - e_1)^2]^{\frac{1}{2}} \quad \text{(A1)}$$

where e_1, e_2 and e_3 are the principal natural 'strains' (i.e. analysis treats the data as though enclave fabrics are initially isotropic). The shape of the fabric ellipsoid is given as the Lodes parameter, v (Hossack, 1968).

$$v = [2(e_2) - e_1 - e_3]/(e_1 - e_3). \quad \text{(A2)}$$

The Lodes parameter ranges from +1.0 to −1.0, with positive values representing flattening fabrics, negative values representing constrictional fabrics, and 0 representing plane fabric geometry.